ZOOLOGICAL SCIENCE 26: 632–638 (2009)

Functional Changes with Feeding in the Gastro-Intestinal Epithelia of the Burmese Python (*Python molurus*)

Cécile Helmstetter[1], Nathalie Reix[1], Mathieu T'Flachebba[1], Robert K. Pope[1], Stephen M. Secor[2], Yvon Le Maho[1] and Jean-Hervé Lignot[1]*

[1]*CNRS, Département d'Ecologie, Physiologie et Ethologie, 23 rue Becquerel, F-67087 Strasbourg cedex 2, France*
[2]*Department of Biological Sciences; Box 870344, The University of Alabama, Tuscaloosa, AL 35487-0344, USA*

The morphology of the digestive system in fasting and refed Burmese pythons was determined, as well as the localization of the proton (H^+, K^+-ATPase) and sodium (Na^+, K^+-ATPase) pumps. In fasting pythons, oxyntopeptic cells located within the fundic glands are typically non-active, with a thick apical tubulovesicular system and numerous zymogen granules. They become active immediately after feeding but return to a non-active state 3 days after the ingestion of the prey. The proton pump, expressed throughout the different fasting/feeding states, is either sequestered in the tubulovesicular system in non-active cells or located along the apical digitations extending within the crypt lumen in active cells. The sodium pump is rapidly upregulated in fed animals and is classically located along the baso-lateral membranes of the gastric oxyntopeptic cells. In the intestine, it is only expressed along the lateral membranes of the enterocytes, i.e., above the lateral spaces and not along the basal side of the cells. Thus, solute transport within the intestinal lining is mainly achieved through the apical part of the cells and across the lateral spaces while absorbed fat massively crosses the entire height of the cells and flows into the intercellular spaces. Therefore, in the Burmese python, the gastrointestinal cellular system quickly upregulates after feeding, due to inexpensive cellular changes, passive mechanisms, and the progressive activation and synthesis of key enzymes such as the sodium pump. This cell plasticity also allows anticipation of the next fasting and feeding periods.

Key words: *Python molurus*, stomach, intestine, morphology, H^+, K^+-ATPase, Na^+, K^+-ATPase

INTRODUCTION

The Burmese python (*Python molurus*) possesses the adaptive capacity to widely regulate gastrointestinal (GI) performance with feeding and fasting (Secor and Diamond, 1995; 1997). This trait, hypothesized to be an adaptation to the python's infrequent feeding habits, is shared by other infrequently feeding snakes and estivating anurans (Secor and Diamond, 2000; Secor, 2005). The adaptive response of the python GI tract is highlighted by the plasticity in form and function of the small intestine. Noted trophic responses of the postprandial python small intestine include the doubling of mass, hypertrophy of the epithelial enterocytes, lengthening of the villi as the prior pseudo-stratified epithelium spreads into a single-layered epithelium, and a five-fold increase in microvillus length (Starck and Beese, 2001; Lignot et al., 2005). Concurrent with the morphological responses is the rapid upregulation of small intestinal function. Within 48 hours after feeding, amino-oligopeptidase activity has tripled and mass-specific rates of amino acid and glucose transport have increased by 5 to 10-fold (Ott and Secor, 2007; Secor and Diamond, 1995, 1997). Upon the completion of digestion, the upregulatory responses are reversed; the enterocytes atrophy, villi shorten, the microvilli retract, and nutrient transport is downregulated (Lignot et al., 2005; Secor and Diamond, 1995). For the Burmese python and other infrequently feeding snakes, the selective advantage of GI downregulation with fasting is reduction in the cost of maintaining the energetically expensive digestive tract during long periods of fasting. This energy saving absorbs the additional cost incurred with postprandial upregulation of the quiescent gut (Secor and Diamond, 2000; Secor, 2001).

Digestion is widely considered to be a very integrative process involving the interactions of a number of different organs and tissues. Concurrent with the small intestine, other organs of the pythons must also experience dramatic regulatory responses in morphology and function with feeding. Although attention in the past has largely focused on trophic and functional responses of the python's small intestine, other studies have shown that the python's heart and stomach upregulate performance with feeding. Cardiac output of pythons increases 4.5–fold during the digestion of meals equalling 25% of the body mass (Secor et al., 2000). In response to similarly sized meals, the python stomach experiences a rapid drop in pH (8 to 2) within 24 h after feed-

* Corresponding author. Phone: +33-3-88-10-69-38;
Fax : +33-3-88-10-69-06;
E-mail: J-H.Lignot@c-strasbourg.fr
doi:10.2108/zsj.26.632

ing and maintains a pH of 1.5 for the 6 to 8 days of gastric digestion (Secor, 2003). Once gastric digestion has finished, the luminal pH returns to being more neutral (Secor, 2003).

Our understanding of stomach function and responses has been gained mainly from studies on mammals (Ogata and Yamasaki, 2000). In the mammalian stomach, parietal cells are responsible for the production of HCL, whereas chief cells secrete the inactive pepsin-precursor, pepsinogen. Both cell types are housed within gastric glands located in the fundic region of the stomach. For non-mammalian vertebrates, it has been found that one cell type, oxyntopeptic cells, is responsible for both tasks (Sedar, 1961; Giraud et al., 1979). The ingestion of food triggers a known collection of morphological and functional responses of the mammalian gastric epithelium. The apical surface becomes greatly expanded due to the fusion of cytoplasmic tubulovesicular membranes (Forte et al., 1980). Pepsinogen, stored within zymogen granules, is released and cleaved to form pepsin, a proteolytic enzyme. At the apical membrane of the parietal cells, H^+/K^+-ATPase, the proton pump, is activated to release H^+ extracellularly to form HCL (with passively released Cl) in the gastric lumen (Forte et al., 1980; Helander and Keeling, 1993). For recently fed pythons, we expect these responses to occur, though at a much greater magnitude. Consider first the gross distension of the python's stomach following the ingestion of a large, intact meal. Secondly, the meal is largely protein and becomes completely broken down (with the exception of hair and feathers) within the stomach. Third, pythons continuously maintain a highly acidic environment within the stomach for days. And finally, upon the completion of digestion, the stomach resumes a collapsed appearance, and acid and presumably pepsinogen production ceases (Secor, 2003). Therefore, we predict that the python stomach experiences dramatic changes in structure and function, as observed for the small intestine.

Nutrient absorption has been studied mainly in snakes by looking at the effects of food composition on the increased metabolic expenditure that occurs in postprandial animals (specific dynamic action; SDA) (Secor et al., 2002; McCue et al., 2005; Grossmann and Starck, 2006; Secor, 2008). The SDA is affected by meal size and temperature but is mostly dependent on meal composition (McCue, 2006). Fat, starch, cellulose, and simple proteins do not affect the Burmese python SDA, nor does a complete protein diet (McCue, 2006). Also, the postprandial response of *Dasypeltis scabra*, an African rhombic egg eater, is the lowest reported for any snake, suggesting that the SDA is determined mainly by gastric function (Grossmann and Starck, 2006). The morphology and function of the intestine has also been studied when different solutions were infused to the animals (Secor et al., 2002). The intestinal upregulation appeared maximal when a nutritionally complete liquid formula or natural diet was given to the snakes.

To further understand structural and functional responses in the python gastrointestinal tract with feeding and fasting, we explored post-feeding changes in morphology of the gastric wall along with gastric proton (H^+/K^+-ATPase) and intestinal sodium (Na^+, K^+-ATPase) pump expression. It appeared that gastric functions are reactivated immediately after feeding due to very rapid changes in the morphology of oxyntopeptic cells. This allows strong acidification of the gastric lumen. This is followed by de novo synthesis of the sodium pump, which is classically located along the basolateral membranes of the oxyntopeptic cells. In the intestine however, this pump is expressed only along the lateral membranes of the enterocytes. In light of these findings, we discuss the processes occurring within the gastric and intestinal linings during the postprandial period.

MATERIALS AND METHODS

Experimental procedures

Sixteen hatchling pythons weighing~100 g each were purchased from commercial breeders (Zooland, Strasbourg, France) and were maintained individually in temperature-controlled tanks (28–30°C) under a 14 h:10 h light-dark cycle. The snakes were fed laboratory mice and rats bi-weekly, with the mass of each meal approximately 25% of the snake's body mass. For the experiment, pythons averaged 661±145 g (mean±1 SE) and were approximately 6 months old. All snakes fasted for 40–50 days but had access to water and were therefore in a postabsorptive state (Secor and Diamond, 1995). A first group of fasting snakes was sacrificed, whereas the others were refed and then sacrificed at different time intervals after feeding: 0.5, 1, 3, or 6 days following their consumption of rat meals equalling 25% of their body mass.

Rats were killed by concussion. The snakes were decapitated and their spinal cord severed, and they were immediately dissected. For each sampling period, samples were collected from a minimum of three snakes. After sacrifice, samples were removed, cleaned of any contents, and weighed. All housing and experimental procedures were conducted under animal care and use protocols approved by the CNRS.

Light microscopy and immunohistochemistry

The walls of the gastric fundic area as well as of the proximal and mid intestine were dissected on ice. One-cm segments were rinsed with ice-cold reptilian ringer's solution and fixed in 3% paraformaldehyde in buffered saline for two hours. Samples were then dehydrated and embedded in paraffin. Gastric and intestinal cross-sections (6 µm) were cut on a Leica RM2125 microtome, put on poly-L-lysine coated glass slides, and used for immunohistochemistry.

For localization of the proton pump, a rabbit anti-H^+,K^+-ATPase polyclonal antibody directed against the C-terminus of the α-subunit of the pig proton pump was used (Chemicon). This antibody has been used successfully in the stomach of the Atlantic stingray *Dasyatis sabina* (Smolka et al., 1994) and in the amphibian *Triturus carnifex* (Liquori et al., 2005). The specificity of this antibody may be attributable to the high degree of evolutionary conservation of the targeted enzyme in the animal kingdom, and in vertebrates in particular.

Monoclonal antibody IgGα5 developed by Dr. D. Farmbrough and raised against the α-subunit of avian Na^+,K^+-ATPase was purchased from the Hybridoma Bank. This antibody recognizes the three α isoforms (α_1, α_2, α_3) and cross-reacts with the Na^+,K^+-ATPase of several fish and arthropod epithelia (Lebovitz et al., 1989; Baumann and Takeyasu, 1993; Baumann et al., 1994; Just and Walz, 1994; Witters et al., 1996; Ziegler, 1997; Lignot and Charmantier, 2001; Lignot et al., 1999, 2005). Like the proton pump, Na^+, K^+-ATPase is also highly evolutioinarily conserved in the animal kingdom, and in vertebrates in particular. The analysis of the amino acid sequence of the sodium pump, for instance, illustrates this point well: the sequence is about 90% similar in birds, fish, and mammals (Kawakami et al., 1985; Schull et al., 1985; Takeyasu et al., 1988).

The protocol established by Lignot et al. (2005) was used for the detection of the two enzymes in the stomach and intestine. Sections were then examined with a fluorescent microscope (Zeiss Axioplan 2 *imaging*) equipped with the appropriate filter set (450–590 nm bandpass excitation filter) and an Axiocam camera.

Western blot analysis

Total proteins from the proximal intestine from pooled fasting (n=3), 1DPF (n=3), and 3DPF (n=3) pythons were isolated from scraped mucosa after centrifugation (90 min, 30000×*g*) in 10 volumes (weight/volume) of ice-cold sample buffer [10 mM Tris-HCl, 10% SDS, 15 mg/mL DTT, 1% protease inhibitor cocktail (Sigma), pH 7.4]. The plasma membrane fractions were isolated by discontinuous sucrose density gradient centrifugation, as described previously (McCartney and Cramb, 1993). Protein concentrations were determined by the bicinchoninic acid method and Western blotting was conducted using standard techniques (Shi and Jackowski, 1998). Proteins (25 μg per lane) were separated by SDS-PAGE in 7% poly-acrylamide gels and electroblotted onto PVDF membranes before processing for immunodetection. The membranes were incubated with the primary antibody (anti-chicken IgGα5, Hybridoma Bank). Control blots were also run simultaneously using equivalent dilutions of pre-immune serum. Membranes were finally incubated with an alkaline phosphatase-conjugated secondary antibody, and the bound antibodies were visualized by incubating the blots in BCIP-NBT (Chemicon). The level of immunoreactivity was then measured as the peak intensity by using an image capture and analysis system (Scion Image Analysis). Results are expressed as relative densitometric units, normalized to the values of Ponceau-stained blots to account for any differences in protein loading among lanes.

Transmission electron microscopy

Small samples of the stomach and proximal intestine were fixed in 2.5% glutarhaldehyde in 0.05 M cacodylate buffer (pH=7.4) for transmission electron microscopy. Samples were subsequently post-fixed in 1% osmium tetroxide, dehydrated in a graded series of ethanol, and embedded in Araldite 502 resin. Semi-thin (≈0.5 μm) and ultra-thin sections (≈90 nm) were respectively placed on poly-L-lysine-coated slides or copper grids. Semi-thin sections were stained with toluidine blue and observed to describe postprandial changes in the cell structure and organization. Ultra-thin sections were stained with uranyl acetate for 30 min and lead citrate for 3 min and examined on a Philips CM 12 electron microscope.

RESULTS

Morphology of the stomach and intestinal lining

Dissections of the stomach showed no strict limit between the esophagus and the stomach, and revealed the presence of a thick pyloric sphincter separating the stomach from the intestine (Fig. 1A). Digestion of the prey appeared to be very rapid, with only hair remaining within the stomach 3 to 6 days after feeding, mainly in the central part of the stomach characterised by deep folds (Fig. 1A). Using the classical Masson's trichrome staining procedure, three main areas were characterised, as follows. 1) The anterior part of the stomach has a lining similar to that seen in the esophagus and is composed of a simple mucus epithelium without gastric glands underneath (Fig. 1B). 2) A clear change is observed in the middle part of the stomach; the gastric lining thickens and presents numerous gland openings (Fig. 1C). Underneath these openings, mucus neck cells are present and are prolonged by elongated glands. This area corresponds to the fundic region. Within the main glandular body, only one cell type could be identified: the so-called "oxyntopeptic cell" located all along the wall of the glands. These cells contribute to gastric juice acidification through H^+ secretion and also to the production of pepsinogen. 3) The pyloric region is composed of a mucus epithelium and presents numerous openings with large glands underneath

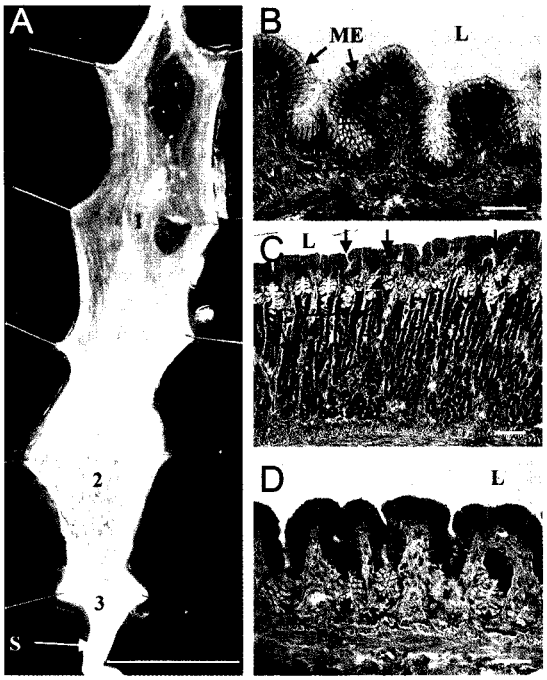

Fig. 1. Histology of the stomach of *Python molurus*. **(A)** Fasting animal. **(B–D)** Anterior, median, and posterior parts of the stomach. Sections were stained using Masson's trichrome protocol. L, lumen; NC, neck cells; ME, mucus epithelium; P, prey; S, pyloric sphincter; SG, sac gland; 1, anterior part of the stomach; 2, fundic area; 3, pyloric area. Arrows, openings of glands. Scale bars, 5 cm (A), 100 μm (B–D).

possessing mucous secreting cells (Fig. 1C).

In the intestine, numerous villi protrude deeply into the intestinal lumen, are lined with an absorbing epithelium, and are composed of typical elongated enterocytes that possess apical microvilli (brushborder) and large basal nuclei (for more explanation, see Starck and Beese, 2001; Lignot et al., 2005). These intestinal villi lack crypts at their base, indicating that most of the cell replication must occur randomly along the epithelium (Helmstetter et al., in press).

Effects of fasting and feeding on stomach and intestinal morphology

Fundic areas of stomach samples taken from fasting snakes present elongated and collapsed glands (Fig. 2A, B). Twelve hours after feeding, fundic glands are shortened (Fig. 2C), their lumens are enlarged, and the crypt wall is thinner than in fasting animals (Fig. 2D). However, three days after feeding, the crypt wall thickens again (Fig. 2E).

At the ultrastructural level, the oxyntopeptic cells of fasting animals possess a basally located nucleus, are packed with secretory vesicles, and present typical non-active ultrastructural features, i.e., a dense apical tubulo-vesicular system along with numerous secretory granules filling the cells (Fig. 2F). The tubulo-vesicular system consists of smooth-surfaced vesicles and tubules. Unlike the mammalian acid-secreting cell, the python oxyntopeptic cell does not contain an intracellular canaliculus invaginated into the cytoplasm from the apical membrane. However, the surface area of the apical membrane presents short digitations (Fig. 2F).

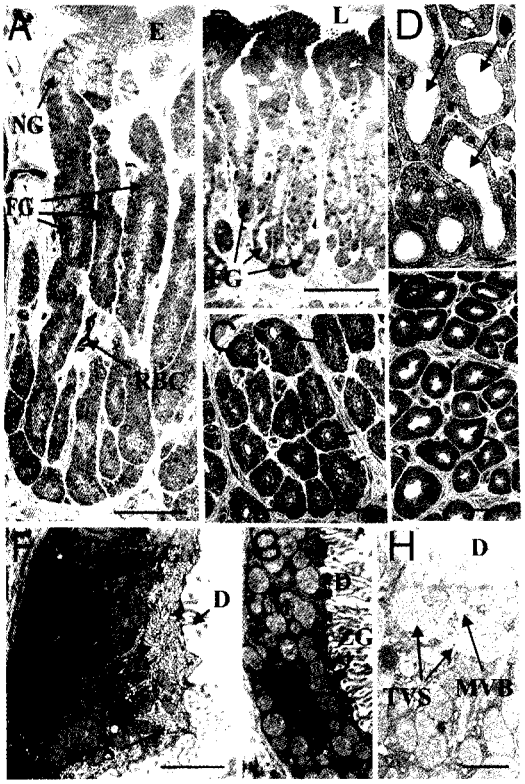

Fig. 2. **(A)** Longitudinal **(B)** and oblique sections of fundic glands of a fasting snake, *Python molurus*. **(C, D)** Cross-sections of fundic glands of a 12 HPF snake. **(E)** Cross section of fundic glands of a 3 DPF snake. Note the shortening of the glands as well as their enlargement and the reduced thickness of the crypt wall immediately after feeding. **(F)** Oxyntopeptic cell of a fasting snake containing a thick apical tubulovesicular system, zymogen granules, and short digitations. **(G)** Typical oxyntopeptic cell of a 12 HPF snake with no tubulovesicular system, few apical zymogen granules, and numerous mitochondria. **(H)** Detail of the apical area of a 3DPF oxyntopeptic cell presenting a non-acid-secreting state and containing multivesicular bodies embedded within the tubulovesicular system. D, digitation; E, epithelium; FG, fundic gland; M, mitochondria; MVB, multivesicular body; N, nucleus; RBC, red blood cells; TVS, tubulovesicular system; ZG, zymogen granules; arrows, enlargement of the lumen inside the fundic glands. Scale bars, 50 μm (A–C); 20 μm (D, E); 2 μm (F–H).

Twelve hours after feeding, oxyntopeptic cells aligned along the walls of the crypts possess numerous mitochondria but fewer zymogen granules. These granules appear mostly at the apical surface of the cells, just underneath the apical digitations that apparently form from complete fusion of the tubulovesicular membranes with the apical membrane surface (Fig. 2G). Three days after feeding, most of the cells already possess the typical non-active ultrastructural features corresponding to the apical tubulo-vesicular system and are also packed with new secretory granules.

In the proximal intestine, enterocytes of the absorbing epithelium also possess a wide plasticity that has already been demonstrated (Starck and Beese, 2001; Lignot et al., 2005). These cells possess very short microvilli and are arranged in a pseudostratified fashion in fasting animals. In refed animals, however, their width rapidly increases, thus inducing a significant increase in villus length and intestinal mass. Contributing to enterocyte hypertrophy is the cellular accumulation of lipid droplets at the tips and edges of the villi.

Effects of fasting and feeding on proton and sodium pumps in the stomach

Gastric sections from 3 DPF snakes incubated with PBS instead of the primary antibody directed against the H^+, K^+-ATPase revealed low background fluorescence from the crypt walls and non-specific staining from red blood cells (Fig. 3A). When incubated with the antibody recognising the H^+, K^+-ATPase, all sections revealed specific staining precisely located within the apical area of the oxyntopeptic cells of the fundic glands (Fig. 3B–D). The mucus epithelium, mucus neck cells, and pyloric glands, however, presented no specific staining. In fasting snakes, the labelling appeared as a thick, diffuse staining within the apical region of non-secreting cells (Fig. 3B). In the 12 HPF and 1 DPF samples, the fluorescence was brighter, thinner, and located at the tip of the cells (Fig. 3C, D). Therefore, it can be considered that the proton pump in these post-feeding animals is relocated along the digitations extending within the lumens of the fundic crypts. The morphological reorganisation appearing in the oxyntopeptic cells of the 3- and 6-day post-feeding snakes and the change observed once again in the proton pump labelling (diffuse thickening of the fluorescence) indicate that the proton pump becomes again sequestered within the tubulovesicular system as soon as 3 days after feeding (Fig. 3E, F).

For the sodium pump, control sections from 3 DPF snakes that were incubated with the antibody-free solution revealed no specific fluorescence from the stomach walls, except for the red blood cells (Fig. 4A). When appropriately incubated with the primary and secondary antibobies, no specific staining was observed in the fundic sections of fasting animals (Fig. 4B) and very faint staining could be seen in the 12 HPF samples (Fig. 4C) This specific staining indicating the presence of the Na^+, K^+-ATPase appeared along the baso-lateral membranes of the oxyntopeptic cells within the fundic region of the stomach with increased intensity from 12 HPF up to 6 DPF (Fig. 4C–F). In the pyloric glands, the intensity of staining increased from 12 HPF up to 3 DPF (Fig. 4G–I).

Expression and localization of Na^+, K^+-ATPase in the intestine

Western blotting on samples from the proximal intestine revealed a specific band that was located as expected around 116 KDa. Expression of the sodium pump increased by 60% in the 1 and 3 DPF samples compared to the fasting snakes (Fig. 5). Within intestinal villi, no staining was detected in fasting animals, but specific immunoreactivity was observed in fed snakes along the lateral membranes of the enterocytes (Fig. 6). The intensity of this staining increased from 12 HPF up to 3 DPF and decreased in the intestine of the 6-day post-feeding snakes (Fig. 6B–F) even though the concentrations of the primary and secondary antibodies remained the same in the various immunolabelling experiments conducted. The immunoreativity was only found above the lateral spaces between enterocytes (Fig. 6E).

DISCUSSION

The onset of refeeding in Burmese pythons has an immediate and noticeable impact on the physiology of the stomach (Secor, 2003) and small intestine (Secor and Diammond,

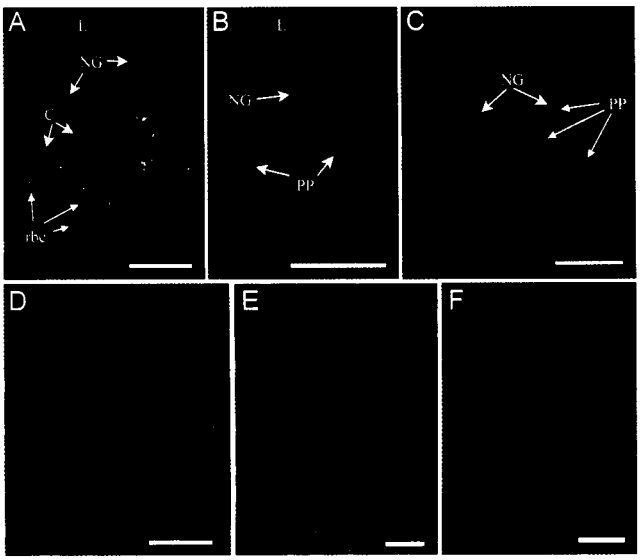

Fig. 3. Immunolabelling of the proton pump within the fundic glands of *Python molurus*. **(A)** Control section incubated with PBS lacking the primary antibody. **(B)** Fasting snake. **(C–F)** 12 HPF, 1 DPF, 3 DPF, and 6 DPF, respectively. C, fundic gland; L, lumen; NG, neck gland; PP, proton pump staining; rbc, red blood cell. Scale bars, 50 μm (A–D); 20 μm (E, F).

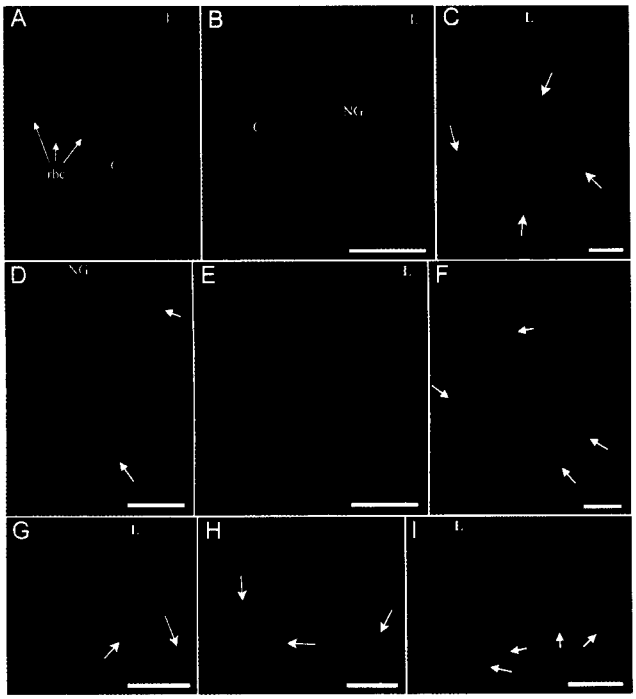

Fig. 4. Immunolabelling of the sodium pump within the fundic crypts of *Python molurus*. **(A)** Control section incubated with PBS lacking the primary antibody. **(B)** Fasting snake. **(C–F)** 12 HPF, 1 DPF, 3 DPF, and 6 DPF, respectively. **(G–I)** Immunolabelling of the sodium pump within the pyloric area of 12 HPF, 1 DPF, and 3 DPF snakes, respectively. Arrows, some of the basolateral membranes positively stained with the antibody; C, fundic gland; L, lumen; NG, neck gland; rbc, red blood cell. Scale bars, 50 μm (A, B, D, E, G, H), 20 μm (C, F, I).

1995; Starck and Beese, 2001, Lignot et al., 2005). Within the stomach, the up-regulation of gastric functions is illustrated by both 1) a sudden acidification of the lumen (within hours),

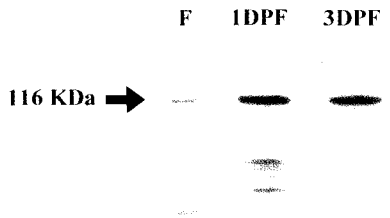

Fig. 5. Na^+/K^+-ATPase expression from the proximal intestinal mucosa of fasting (lane 1), 1 day postfeeding (lane 2), and 3 days postfeeding (lane 3) *Python molurus*. Each lane represents a pool of three snakes. Note that the main band is located at 116 KDa, as expected for the α5 antibody.

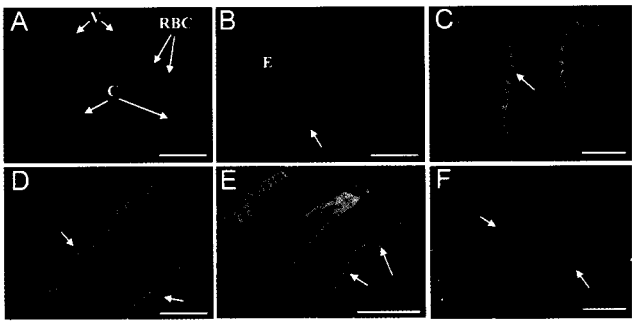

Fig. 6. Na^+/K^+ ATPase immunohistochemistry for proximal intestinal villi of *Python molurus*. **(A)** Fasting snake. **(B–D)** Snakes 12 hours, 1 day, and 3 days post-feeding, respectively. **(E)** Close-up view of the intestinal epithelium of a 3 days post-feeding snake. **(F)** Immunostaining of a 6-day post-feeding snake. Arrows indicate positive staining. Note the strong staining along the lateral membranes in refed animals (arrows). C, chorion; E, epithelium; RBC, red bllod cells; V, intestinal villus. Scale bars, 50 μm.

despite the large buffering capacity of the meal, and 2) the neutral pH values maintained for months in the stomach of fasting snakes (Secor, 2003). This reactivation of the main gastric functions must concur with a sudden cellular and morphological appraisal. This is mainly achieved through the plasticity of the oxyntopeptic cells, as observed in this study. These cells are located within simple tubular glands located in the chorion of the fundus. Unlike in mammals, these cells do not have intracellular canaliculi (deep invaginations of the apical plasma membrane) lined by digitations. However, they possess an apical intracellular tubulovesicular system that is typical of non-secretory cells, and numerous mitochondria and secretory granules (zymogen granules), as seen with fasting snakes. Immediately after feeding, the fundic glands are enlarged, and the ocxyntopeptic cells aligned along the wall of the glands flush their secretions within the crypt lumen. At that time, these cells are very active, as illustrated by the presence of numerous mitochondria and elongated digitations. Also, the intracellular tubulovesicular system has disappeared, suggesting therefore that the tubulovesicles are storage forms for membranes, thus contributing to the increase in surface area of the active cells. This apical reorganisation enables the proton pump to release HCl from the cells into the gastric crypts. This enzyme is sequestered in the tubulovesicular system dur-

ing fasting bouts and is functional immediately after feeding, i.e., as soon as the proton pump faces the luminal side. Also, the sodium pump, typically located along the basolateral membranes of the cells, becomes activated by feeding. Functioning proton pumps drive a huge demand for ATP conversion to ADP+Pi, especially at the apical plasma membrane. Oxygen and substrates to regenerate ATP, however, enter the cell at the basal surface. The flattening of the oxyntopeptic cells may therefore arise not only because of the reshaping of the apical area of the cell and the flushing through the apical side of the zymogen granules, but also in order to limit the distance between apical and basal surfaces. This sudden gastric reactivation, however, is shortly followed by the shutting down of the system. Indeed, 3 days after feeding, most of the cells again possess typical non-active ultrastructural features corresponding to the formation of the apical tubulo-vesicular system and the packing of zymogen granules in the cytoplasm of the oxyntopeptic cells, and it is only after this active period that cell renewal occurs in the neck region of the fundic glands (Helmstetter et al., in press). Before becoming fully functional these new cells will then have to migrate either along the mucus epithelium or within the crypts. These results clearly indicate that digestion of the prey and cell renewal are two mechanisms occurring during the postprandial period but which are well separated during that time. Cell proliferation is also increased in the intestine during the postprandial period (Secor et al., 2000; Starck and Beese, 2001; Helmstetter et al., in press). This process along with protein synthesis, as seen with the sodium pump in the stomach and small intestine (this study), must play a significant role in the general response of the digestive system to feeding, as usually measured by using the specific dynamic action (Mc Cue, 2006; Secor, 2008).

It is now well established that within the intestinal mucosa, cells of fasting pythons are arranged in a pseudostratified fashion with their basolateral membranes containing highly folded regions interlocking tightly with neighbouring cells. Consequently, intercellular spaces are absent in fasting pythons (Starck and Beese, 2001; Lignot et al., 2005). However, in fed animals, the mucosa becomes monolayered with numerous intracytoplasmic lipid droplets accumulating within the enterocytes (Starck and Beese, 2001), mostly located at the tip and along the thin edges of the villi (Lignot et al., 2005). This massive lipid uptake by the enterocytes induces a large widening of the intercellular spaces that must be filled with chylomicrons (Starck and Beese, 2001; Lignot et al., 2005). Therefore, the presence of the sodium pump at the tip of these large intercellular spaces must be a key adaptation in order to maximise nutrient uptake. Furthermore, this is the first time that this highly conserved integral membrane protein — usually located along the basal as well as lateral membranes of polarised cells — is reported to be located solely along the lateral sides of the enterocytes. This is in contrast with a more classical localization of this enzyme in the gastric cells (this study; Dunbar and Caplan, 2001) and intestinal enterocytes (Stirling, 1972; Seidelin et al., 1999; Dunbar and Caplan, 2001; Giffard-Mena et al., 2006). The presence of the sodium pump along the lateral membranes of the enterocytes, i.e., above the lateral spaces, may therefore represent a compromise between water and solute transport by this enzyme from the intestinal lumen into the general circulation and the massive lipid uptake that operates during the postprandial period through the apical brush border of the cells down to the lateral spaces. The high osmolarity in the intercellular spaces between adjacent enterocytes must drive paracellular water diffusion through the tight junctions, as well as transcellular water transport from the intestinal lumen, into the intercellular spaces in response to the osmotic gradient created by sodium. Therefore, the 'standing gradient theory' (Diamond and Bossert, 1967) could potentially be applied to the intracellular and lateral spaces within this fluid-transporting epithelium as local osmotic coupling spaces, especially because of the proximity of the sodium pumps near the tight junctions (Larsen et al., 2009).

In order to complete the study, especially at the onset of the gastric upregulation within the first few hours after the swallowing of the prey, it would be advantageous to measure the activity of carbonic anhydrase within the gastric lining. The regulation of gastric secretion, tightly controlled by positive regulators and negative feedback mechanisms, should also be monitored. Gastric acid production is regulated by both the autonomic nervous system and several hormones. The parasympathetic nervous system, via the vagus nerve, and hormones such as gastrin must stimulate the oxyntopeptic cell to produce gastric acid, and both systems must directly act on the oxyntopeptic cells. The inhibitory action of vasoactive intestinal peptide, cholecystokinin, and secretin on gastric juice production could also be tested.

To conclude, this study indicates that in the Burmese python, the gastrointestinal system can quickly upregulate after feeding. In the stomach, although the proton pump is expressed in fasting animals, it is sequestered in the apical tubulovesicular system of the oxyntopeptic cells and may not therefore be functional. However, immediately after feeding, the proton pump can readily be active due to a rapid morphological change in the oxyntopeptic cells. This along with the diffusion of gastric enzymes into the lumen then allows strong acidification of the gastric lumen and digestion of the prey. During that time, other enzymes such as the sodium pump are synthesized in the fundic and pyloric regions of the stomach. In turn, this is rapidly followed by a switch back to a non-active state for oxyntopeptic cells, also filling up with secretory reserves. In the intestine, refeeding triggers de novo synthesis of the sodium pump. This enzyme must then switch on the activity/synthesis of several facilitated membrane transport proteins, which import glucose, amino acids, and other nutrients into the cell. The activity of the sodium pump must also create an osmotic gradient that drives the absorption of water from the intestinal lumen.

ACKNOWLEDGMENTS

We thank C. Arbiol for technical assistance. Financial support for this study was provided by the CNRS Life Science Department to R.K Pope, and by the Scientific Committee of the University Louis Pasteur.

REFERENCES

Baumann O, Takeyasu K (1993) Polarized distribution of Na, K-ATPase in honeybee photoreceptors is maintained by interaction with glial cells. J Cell Sci 105: 287–301

Baumann O, Lautenschläger B, Takeyasu K (1994) Immunolocalization of Na, K-ATPase in blowfly photoreceptor cells. Cell Tissue Res 275: 225–234

Coulson RA (1985) Delayed protein synthesis in the alligator following carbonic anhydrase inhibition. Comp Biochem Physiol A 82: 43–47

Diamond JM, Bossert WH (1967) Standing-gradient osmotic flow. A mechanism for coupling of water and solute transport in epithelia. J Gen Physiol. 50: 2061–2083

Duman JG, Pathak NJ, Ladinsky MS, McDonald KL, Forte JG (2002) Three-dimensional reconstruction of cytoplasmic membrane networks in parietal cells. J Cell Sci 115: 1251–1258

Dunbar LA, Caplan MJ (2001) Ion pumps in polarized cells: sorting and regulation of the Na^+, K^+- and H^+, K^+-ATPases. J Biol Chem 276: 29617–29620

Forte JG, Machen TE, Obrink KJ (1980) Mechanisms of gastric H^+ and Cl^- transport. Annu Rev Physiol 42: 111–126

Giffard-Mena I, Charmantier G, Grousset E, Aujoulat F, Castille R (2006) Digestive tract ontogeny of *Dicentrarchus labrax*: Implication in osmoregulation. Dev Growth Differ: 48: 139–151

Giraud AS, Yeomans ND, St John DJ (1979) Ultrastructure and cytochemistry of the gastric mucosa of a reptile, *Tiliqua scincoides*. Cell Tissue Res 197: 281–294

Grossmann J, Starck JM (2006) Postprandial responses in the African rhombig egg eater (*Dasypeltis scabra*). Zoology 109: 310–317

Helander HF, Keeling DJ (1993) Cell biology of gastric acid secretion. Bailliere Clin Gastroenterol 7: 1–21

Helmstetter C, Pope RK, T'Flachebba M, Secor SM, Lignot J-H (2009) The effects of feeding on cell morphology and proliferation of the gastrointestinal tract of juvenile Burmese pythons (*Python molurus*). Can J Zool, in press

Just F, Walz B (1994) Immunocytochemical localization of Na^+/K^+-ATPase and V-H^+-ATPase in the salivary glands of the cockroach, *Periplaneta americana*. Cell Tissue Res 278: 161–170

Kawakami K, Noguchi S, Noda M, Takahashi H, Ohta T, et al. (1985) Primary structure of the α-subunit of *Torpedo californica* (Na^++K^+)-ATPase deduced from c-DNA sequence. Nature 316: 733–736

Larsen EH, Willumsen NJ, Møbjerg N, Sørensen JN (2009) The lateral intercellular space as osmotic coupling compartment in isotonic transport. Acta Physiol 195: 171–186

Lebovitz RM, Takeyasu K, Fambrough DM (1989) Molecular characterization and expression of the (Na^++K^+)-ATPase alpha-subunit in *Drosophila melanogaster*. EMBO J 8: 193–202

Lignot JH, Charmantier G (2001) Immunolocalization of Na^+, K^+-ATPase in the branchial cavity during the early development of the European lobster *Homarus gammarus* (Crustacea, Decapoda). J Histochem Cytochem 49: 1013–1023

Lignot JH, Charmantier-Daures M, Charmantier G (1999) Immunolocalization of Na^+, K^+-ATPase in the organs of the branchial cavity of the European lobster *Homarus gammarus* (Crustacea, Decapoda). Cell Tissue Res 296: 417–426

Lignot JH, Helmstetter C, Secor SM (2005) Postprandial morphological response of the intestinal epithelium of the Burmese python (*Python molurus*). Comp Biochem Physiol A 141: 280–291

Liquori GE, Zizza S, Mastrodonato M, Scillitani G, Calamita G, Ferri D (2005) Pepsinogen and H, K-ATPase mediate acid secretion in gastric glands of *Triturus carnifex* (Amphibia, Caudata). Acta Histochem 107: 133–141

McCartney S, Cramb G (1993) Effects of a high-salt diet on hepatic atrial natriuretic peptide receptor expression in Dahl salt-resistant and salt-sensitive rats. J Hypertens 11: 253–262

McCue MD (2006) Specific dynamic action: a century of investigation. Comp Biochem Physiol A: 144: 381–394

McCue MD, Bennett AF, Hicks JW (2005) The effect of meal composition on specific dynamic action in burmese pythons (*Python molurus*). Physiol Biochem Zool 78: 182–192

Ogata T, Yamasaki Y (2000) Morphological studies on the translocation of tubulovesicular system toward the intracellular canaliculus during stimulation of the gastric parietal cell. Microsc Res Tech 48: 282–292

Ott BD, Secor SM (2007) Adaptive regulation of digestive performance in the genus *Python*. J Exp Biol 210: 340–356

Schull GE, Schartz M, Lingrel JB (1985) Amino-acid sequence of the catalytic subunit of the (Na^++K^+) ATPase deduced from a complementary DNA. Nature 316: 691–695

Secor SM (2001) Regulation of digestive performance: a proposed adaptive response. Comp Biochem Physiol A 128: 565–577

Secor SM (2003) Gastric function and its contribution to the postprandial metabolic response of the Burmese python, *Python molurus*. J Exp Biol 206: 1621–1630

Secor SM (2005) Physiological responses to feeding, fasting and estivation for anurans. J Exp Biol 208: 2595–2608

Secor SM (2008) Specific dynamic action: a review of the postprandial metabolic response. J Comp Physiol B 179: 1–56

Secor SM, Diamond J (1995) Adaptive responses to feeding in Burmese pythons: pay-before pumping. J Exp Biol 198: 1313–1325

Secor SM, Diamond J (1997) Effects of meal size on post-prandial responses for juvenile Burmese pythons (*Python molurus*). Am J Physiol 272: R902–R912

Secor SM, Diamond J (2000) Evolution of regulatory responses to feeding in snakes. Physiol Biochem Zool 73: 123–141

Secor SM, Whang EE, Lane JS, Ashley SW, Diamond J (2000) Luminal and systemic signals trigger intestinal adaptation in the juvenile python. Am J Physiol 279: G1177–G1187

Secor SM, Lane JS, Whang EE, Ashley SW, Diamond J (2002) Luminal nutrient signals for intestinal adaptation in pythons. Am J Physiol 283: G1298–G1309

Sedar AW (1961) Electron microscopy of the oxyntic cell in the gastric glands of the bullfrog, *Rana catesbiana*. II. The acid-secreting gastric mucosa. J Biophys Biochem Cytol 10: 47–57

Seidelin M, Madsen SS, Byrialsen A, Kristiansen K (1999) Effects of Insulin-like Growth Factor-I and Cortisol on Na^+, K^+-ATPase expression in osmoregulatory tissues of brown trout (*Salmo trutta*). General Comp Endocrinol 113: 331–342

Shi Q, Jackowski G (1998) One-dimensional polyacrylamide gel electrophoresis. In "Gel Electrophoresis of Proteins. A Practical Approach" 3rd ed Ed by BD Hames, Oxford University Press, Oxford, pp 1–52

Smolka AJ, Lacy ER, Luciano L, Reale E (1994) Identification of gastric H, K-ATPase in an early vertebrate, the Atlantic stingray *Dasyatis sabina*. J Histochem Cytochem 42: 1323–1332

Starck JM, Beese K (2001) Structural flexibility of the intestine of Burmese python in response to feeding. J Exp Biol 204: 325–335

Stirling CE (1972) Radioautographic localisation of sodium pump sites in rabbit intestine. J Cell Biol 53: 704–714

Takeyasu K, Tamkun MM, Renaud KJ, Fambrough DM (1988) Ouabain sensitive (Na^++K^+)-ATPase activity expressed in mouse L cells by transfection with DNA encoding the α-subunit of an avian sodium pump. J Biol Chem 263: 4347–4354

Witters H, Berckmans P, Vangenechten C (1996) Immunolocalization of Na^+, K^+-ATPase in the gill epithelium of rainbow trout, *Oncorhynchus mykiss*. Cell Tissue Res 283: 461–468

Ziegler A (1997) Immunocytochemical localization of Na^+, K^+-ATPase in the calcium-transporting sternal epithelium of the terrestrial isopod *Porcellio scaber* L. (Crustacea). J Histochem Cytochem 45: 437–446

(Received January 19, 2009 / Accepted June 23, 2009)